A Study of Design and Control of a Quadruped Walking Vehicle

Shigeo Hirose

The International Journal of Robotics Research 1984 3: 113
DOI: 10.1177/027836498400300210

Shigeo Hirose
Department of Physical Engineering
Tokyo Institute of Technology
2-12-1 Ookayama, Meguro-ku
Tokyo, Japan

A Study of Design and Control of a Quadruped Walking Vehicle

Abstract

The paper addresses some of the fundamental problems of energy efficiency, design, and adaptive gait control of quadruped walking vehicles. The design principle of a leg called a gravitationally decoupled actuator (GDA) is shown to be indispensable for realizing energetically efficient walking motion. A novel mechanism, the three-dimensional Cartesian-coordinate pantograph (PANTOMEC), which follows the GDA principle and has a lightweight structure, is introduced. A constructed quadruped walking vehicle model is then described: the walking vehicle has the PANTOMEC leg mechanisms, eight tactile sensors and a posture detector, and is hierarchically controlled by a microcomputer. Comparatively high energy efficiency and a certain degree of terrain adaptability is demonstrated. It is thus shown that a practical walking vehicle can be designed using the proposed method.

The adaptive gait control problem is formalized, and an algorithm for terrain-adaptive gait control is presented. By computer simulation, it is shown that the algorithm produces an efficient gait while avoiding "deadlock" positions in negotiating terrain. The algorithm is shown to be applicable for the control of future quadruped walking vehicles with visual sensors.

1. Introduction

Cursorial animals are considered to have off-road mobility superior to that of conventional wheeled or tracked vehicles. This fact has motivated attempts to realize an artificial walking vehicle that have spanned roughly the past 20 years. During this time, there have been three distinct phases in the study of walking vehicles.

The International Journal of Robotics Research,
Vol. 3, No. 2, Summer 1984,
0278-3649/84/0200113-21 $05.00/0.

The first phase centered on the study of walking vehicles with mechanical coordination. By use of cam and link mechanisms, synchronized leg motion was realized. Some of the walking vehicles constructed (Shigley 1960; Baldwin 1966) demonstrated comparatively high mobility. These vehicles played an important role in awakening people to the possibility of walking vehicles as an alternative to conventional wheeled or tracked vehicles in land locomotion. The efficiency of these vehicles was low, however, and adaptability to irregular terrain was very limited. As terrain adaptability is the distinctive feature of walking vehicles, these first-generation studies did not exploit the real advantage of walking vehicles.

The rapid advance of computer technology and the difficulty of manual control of a human-carrying, quadruped walking vehicle (Mosher 1968) caused the study of walking vehicles to enter its second phase. In the second phase, a generalized walking vehicle with multiple degrees of freedom was considered, and the coordinated control of the legs by computer was investigated. Pioneering work was conducted in the United States (McGhee and Frank 1968; McGhee et al. 1978; McGhee and Iswandhi 1979) and in the Soviet Union (Kugushev and Jaroshevskij 1975), especially in the area of hexapod vehicles. This second phase of research on walking vehicles was also unsatisfactory, because the energetic aspect of the vehicles was given very little consideration.

A manipulator, or the industrial realization of a mechanical hand, can perform its function even if its energy efficiency is low, because the controller, power source, and actuators can be separated from the manipulator itself. In contrast, the walking vehicle, or the industrial realization of a mechanical leg, cannot fulfill its function with low energy efficiency, because it has to carry all its driving and control units in addition to its body to be an autonomous locomotor.

The third phase of walking-vehicle research begins with the recognition of this fact. The third generation of walking vehicles is characterized by the systematic consideration of both energy efficiency and control.

This paper summarizes the author's research to date on quadruped walking vehicles. It is hoped that this research will stimulate further third-phase studies of walking vehicles.

The energy efficiency of walking vehicles is discussed first. Energy efficiency in walking motion is hard to achieve because both body-support forces and propulsive forces are delivered by the driving joint actuators. The gravitationally decoupled actuator (GDA) principle is introduced here as one solution to this problem. A leg mechanism using a three-dimensional Cartesian-coordinate pantograph mechanism (PANTOMEC) is proposed that follows the GDA principle and realizes a lightweight leg structure.

Next, a constructed quadruped walking vehicle incorporating the PANTOMEC, tactile sensors, and a posture detector is described. The reflex-motion-control algorithm is explained, and the results of some (successful) walking experiments are stated.

The adaptive-gait-control problem is discussed and formalized for a quadruped walking vehicle. A hierarchical algorithm for walking motion is described, and the principles involved in the adaptive-gait-control level of the hierarchy are presented in detail. The results of a computer simulation of adaptive walking motion, using the algorithm, are also given. Finally, some of the unsolved problems for walking vehicles are summarized.

2. Energy Efficiency and the Design of Walking Vehicles

2.1. Evaluation of the Energy Efficiency of a Locomotor

Gabrielli and von Karman (1950) showed that specific resistance, ϵ, is an appropriate measure of energy efficiency in a locomotion system. Specific resistance is defined as

$$\epsilon = \frac{E}{WL}, \tag{1}$$

Table 1. Classification of Specific Resistance ϵ According to the Definition of the Energy E and Weight W in (Eq. 1)

Energy \ Weight	Total	Net
Total	$\epsilon_{\text{type 1}}$	$\epsilon_{\text{type 2}}$
Net	$\epsilon_{\text{type 3}}$	$\epsilon_{\text{type 4}}$ (ϵ^*)

where E is the energy consumed during locomotion; W is the weight of the locomotor; and L is the distance of locomotion. The specific resistance is a nondimensional quantity and is suitable for general discussion. For example, human walking at normal speed has a specific resistance of 0.3 to 0.4. The specific resistance of a locomotor moving horizontally at a constant speed is 0, provided that the motion actuators are perfectly efficient and frictional resistance is neglected. When the object is moving straight up, the specific resistance is 1. In the case of an object sliding on a floor with frictional coefficient μ, the specific resistance is μ. The above definition of specific resistance contains some ambiguity, mainly owing to the definitions of weight, W, and consumed energy, E. Thus, in 1979, Hirose and Umetani proposed to classify specific resistance into the four types shown in Table 1.

Specific resistance of type 1 is the definition primarily used until now: that is, E is the total energy consumed by the system, and W is the total weight. The type 1 definition is useful in making general comparisons of many types of locomotors from catalogued data (Gabrielli and von Karman 1950; Park 1962). Specific resistance of type 2 also takes E to be the total energy consumed by the system, but W is taken as the weight of the payload only. Therefore, the type 2 definition is suitable for the realistic evaluation of a transporter. For example, specific resistance of type 2 reveals the inefficiency of a walking vehicle, even if it is powerful and moves fast, when the leg-driving mechanism occupies the whole system and leaves no room for a payload.

Specific resistance of type 3 corresponds to the net cost of transport used in studying the physiology of animal locomotion (Taylor 1973; Goldspink 1977).

Table 2. Classification of Actuators According to Energy Flow in the Three Work Modes

Work mode / Actuator	Positive	Isometric	Negative	Example
Type 1	+	+	+	Muscle
Type 2	+	0	0	Motor with brake
Type 3	+	0	−	Motor with regenerating brake

In this case, W is the total weight of the system, while E is the energy used in locomotion (energy used by the animal for other functions, such as basal metabolism, is not included in this definition of E). Formerly, the energy efficiency of animal locomotion was measured in such units as $ml(O_2)/kg \cdot m$ or $cal/kg \cdot m$, and $mole(O_2)/kg \cdot m$, $m^3(O_2)$, or $joule/kg \cdot m$ in SI units. It is obvious, however, that a nondimensional quantity is more appropriate for making general comparisons. The author thus proposed the use of the nondimensional specific resistance of type 3 in the field of physiology.

The specific resistance of type 4, henceforth denoted by ϵ^*, is the most appropriate type for the strict evaluation of transporter efficiency. In the definition of ϵ^*, W is taken to be the weight of the payload and E the energy consumed by the locomotor; the author recommends the use of ϵ^* for evaluating the efficiency of walking vehicles.

2.2. Actuator Characteristics and the Energy Efficiency of Legged Motion

Actuators are classified into three groups, according to their qualitative nature, as shown in Table 2 (Hirose and Umetani 1979). The classification is based on the direction of energy flow in the three relevant work modes, namely (1) the positive work mode, when the actuator must supply a force or torque in the direction in which a member is moving; (2) the isometric mode, when the actuator must supply a force or torque, but no motion is produced; and (3) the negative work mode, when the actuator supplies a force or torque opposing the motion of a member.

A type 1 actuator is one that consumes energy during all work modes and is the least efficient. Muscles can be considered as type 1 actuators. Muscles, while ideal in many other respects, are not ideal actuators from the standpoint of energy flow. The type 2 actuator is one that consumes energy only in the positive work mode; during other work modes no energy is used (or produced). An electric motor with a brake or self-lock reduction gear is an example of this type of actuator. The type 3 actuator is the ideal actuator: it recovers energy during the negative work mode and requires no energy in the isometric mode. There have been many attempts to realize type 3 actuators. A flywheel generator, an elastomeric regenerative braking system (Hoppie 1979), and a specialized hydraulic actuator (Nakano et al. 1982) have all been proposed. In the electric motors used in railroad locomotives, dynamic braking regenerates some of the negative energy. Because of inefficiency and mechanical complexity, however, none of these actuators is yet practical for the actuator system of a walking vehicle.

This classification of actuators reveals a fundamental inefficiency of walking vehicles (Hirose and Umetani 1979). Figure 1A shows the leg motion of a walking vehicle moving to the right (the direction of v). As the vehicle moves to the right, the relative position of the leg changes from A to B to C, and the knee joint follows the trajectory indicated by the arrow. (Note that it is the vehicle body that moves, and not the foot.)

At the hip joint H, the torque produced by the force of reaction f at foot F is counterclockwise. The actuator supplies an opposing clockwise torque. During the motion from configuration A to B, the angular motion of upper leg, HK, about the hip, H, is counterclockwise; thus the hip actuator is in the negative work mode (clockwise torque and counterclockwise motion). During the motion from B to C, both the angular motion of HK and the supplied torque at B are clockwise, so the actuator at H is in the positive work mode. At the knee joint, K, the situation is reversed: the knee actuator is in the positive work mode from A to B, and the negative work mode from B to C.

If type 1 or type 2 actuators are used in the joints, the negative work cannot be recovered and a great amount of energy is lost. This situation is illustrated in

Fig. 1. A. Diagram of leg during locomotion. B. Plot of potential energy loss during legged motion.

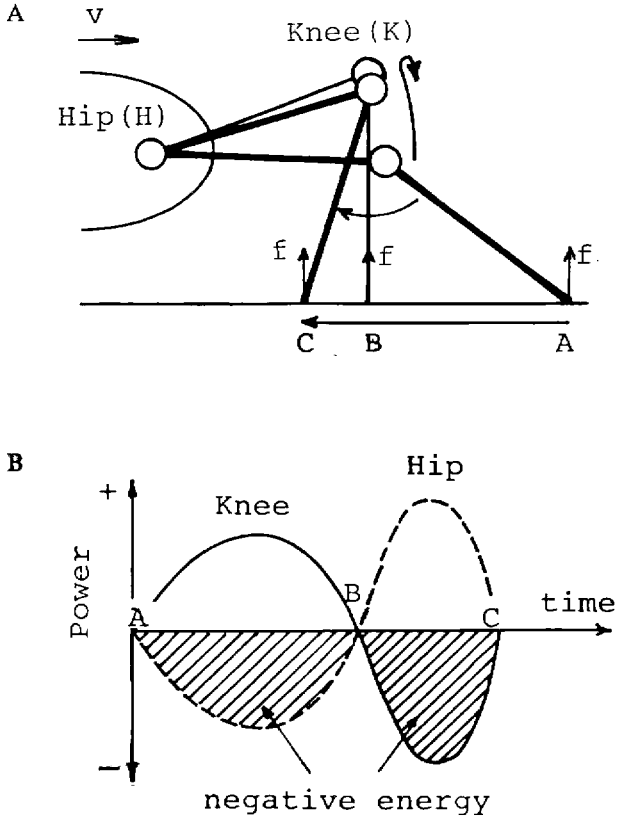

Fig. 1B. Note that energy loss occurs even if the body's center of gravity maintains constant velocity and horizontal motion, and if the kinematic effects of the legs can be neglected.

This discussion reveals a fundamental disadvantage of legged motion. This is not the kind of problem that can be solved by the introduction of a self-lock mechanism or a type 2 actuator, because even if the type 2 actuator eliminated the energy lost in maintaining static posture, it would consume energy as soon as the body moved. Thus a type 3 actuator is indispensable for efficiently realizing the kind of leg mechanism described above and shown in Fig. 1. As previously stated, such an actuator is not now available for a walking vehicle. A new type of leg mechanism, which provides a partial solution to this problem, is presented in Section 2.3.

Fig. 2. Gravitationally decoupled actuator systems. A. Locking type GDA. B. Pantograph mechanism.

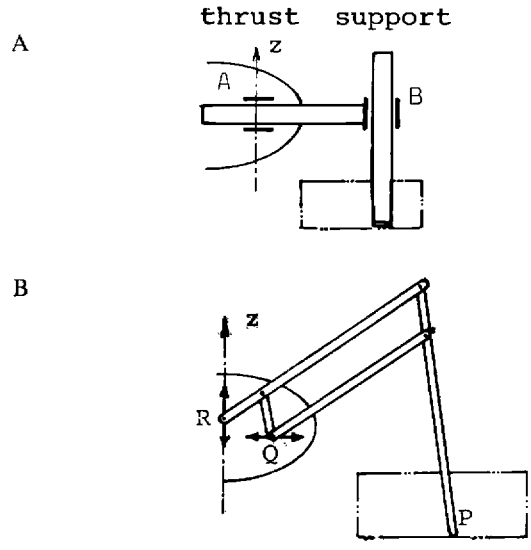

2.3. Introduction of a Gravitationally Decoupled Actuator System

A simple solution to the problem of Section 2.2 is to introduce the leg geometry shown in Fig. 2A (Hirose and Umetani 1978; 1980*a*; 1980*b*). In this configuration, one actuator is locked while the other is moving; hence, with the use of type 2 actuators, energy is consumed by the leg mechanism only in the positive work mode. This is because the actuators are geometrically decoupled between the gravitational direction and its perpendicular direction. This type of actuator system is referred to herein as a gravitationally decoupled actuator Figure 2B shows a GDA leg configuration making use of a pantograph mechanism. The pantograph mechanism magnifies the motion of the vertical and horizontal linear actuators R and Q. The configuration of Fig. 2B has the same decoupling property as in Fig. 2A. Furthermore, it permits a wide reachable area and the lightweight leg structure desirable in a walking vehicle. The mechanism has already been used in a quadruped walking vehicle model (Ikeda et al. 1973); but its energy efficiency, discussed here, does not seem to have been a prime consideration in the model's design. Recently, Waldron and Kinzel (1981) proposed a new leg configuration based on the same design criterion set forth in this paper.

In order to achieve flexibility in gait selection, the leg should have three-dimensional freedom of motion.

Fig. 3. A. Three-dimensional Cartesian-coordinate pantograph mechanism (PANTOMEC). B. Ankle-control mechanism.

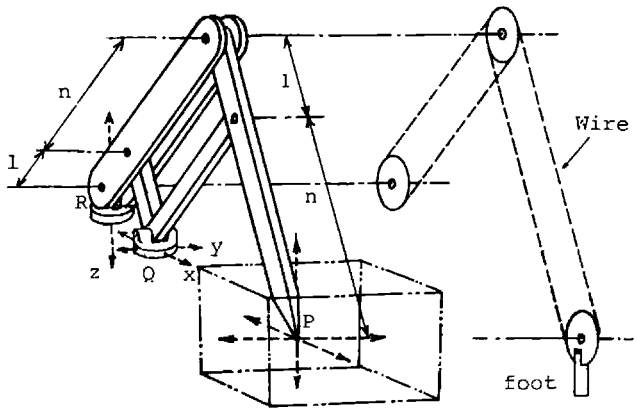

An easy way to realize three-dimensional mobility is to allow the mechanism of Fig. 2 to rotate about a vertical axis to produce cylindrical coordinate motion. The new pantograph mechanism introduced by Hirose and Umetani (1978) permits three-dimensional Cartesian-coordinate motion. This mechanism, called PANTOMEC, is driven by three linear actuators at joints Q and R, as shown in Fig. 3A. The linear actuators and joints Q and R are connected by joints free to rotate around the vertical axis, Z. The PANTOMEC has all the advantages of the two-dimensional pantograph mechanism discussed above (Fig. 2) and in addition has three-dimensional freedom of motion. Since the basic motion of walking is more easily described in Cartesian coordinates than in cylindrical coordinates, the PANTOMEC is also desirable from the standpoint of controllability.

The introduction of a gravitationally decoupled actuator system such as shown in Figs. 2 and 3 diminishes the potential energy loss of walking motion described in Section 2.2. The potential energy loss occupies a major part of the total energy loss in normal walking motion. In a simulation study, it was estimated that the PANTOMEC reduced energy loss by 80% at a walking speed of 5 km/h and a stride 0.6 times the leg length (Hirose and Umetani 1979). The introduction of a decoupled leg geometry is thus of great value in improving the efficiency of vehicular walking motion. At high walking speeds, however, kinematic energy losses in leg motion become significant, and a type 3 actuator becomes indispensable. Waldron and Kinzel (1981) and Nakano et al. (1982) have already begun research into this problem.

3. Preliminary Model of a Walking Vehicle

3.1. Description of an Existing Walking Vehicle

Figure 4 shows a quadruped walking vehicle constructed at the Tokyo Institute of Technology using the PANTOMEC (Hirose and Umetani 1980*c*); the model is referred to as Perambulating Vehicle II (PVII). PVII has a total weight of 10 kg and leg length of 870 mm. Each leg contains 3 dc servo motors (12 motors in all) with 2 W of output power each, and two contact sensors at the bottom and around the sole of each foot (eight contact sensors in all). In addition to the PANTOMEC, each leg includes a parallelogram mechanism (see Fig. 3B) to maintain vertical orientation at the ankles. The ankle-control mechanism consists of three pulleys: one is fixed at the hip joint, another is on the knee joint and is free to rotate around it, and the third is fixed to the ankle joint. These pulleys are connected together by wire loops. This mechanism allows for a lightweight and easily controllable leg, just as the PANTOMEC does. A more sophisticated three-dimensional parallelogram mechanism is discussed elsewhere (Hirose and Umetani 1981).

3.2. Reflex-Motion Regulation System

A microcomputer is used to implement a hierarchical control system, that is, gait control (corresponding to level B of Fig. 9), posture and motion regulation (level C of Fig. 9), and transfer of commands to walking servomechanisms (data transmission). The hierarchical tasks are performed on a time-sharing basis.

In the control system, the gait command is fixed and preassigned. Adaptivity to uneven terrain comes from the basic motion-regulation system at level C of the hierarchy (see Fig. 9). This section discusses the most important part of the control system in PVII: the basic motion-regulation system, which corresponds to reflex motion in biological systems.

3.2.1. The Regulation of Body Height

The objective of body-height regulation is to keep the body at a desired height while it is walking on a

Fig. 4. Quadruped walking vehicle, PVII. A. Crawl gait. B. Bottom view. C. Adaptive walking on stairs, using tactile sensors. D. Elevated posture.

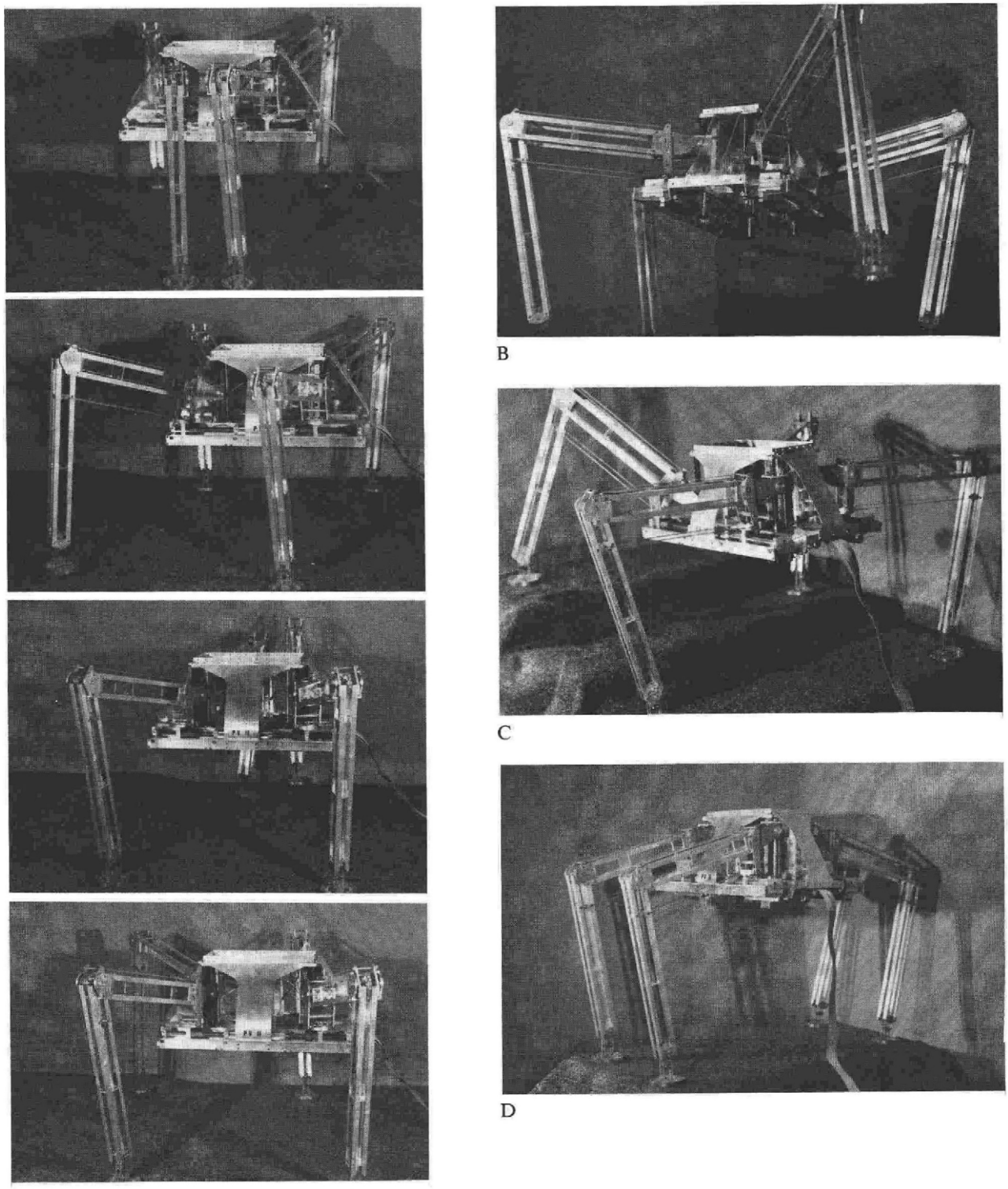

rugged surface. The ideal form of this regulation would be to use a visual sensor to foresee the topography and adjust the body height accordingly. The body height could then be controlled smoothly. At present, however, motion regulation is performed without the aid of a visual sensor and regulates the height of the body using the legs' height signals.

In this regulation, the average height of the supporting legs is measured first, and the body height then adjusted to keep the average foot height at a preassigned value, H. The height, H, is designed to be adjusted by a higher control level, according to the terrain. For example, when the vehicle is walking in bush, the value of H should be larger; and when it is walking on slippery ground, the value of H should be made smaller to effect greater stability. In Fig. 4D, a posture for a high value of H is shown.

3.2.2. *Postural Regulation of the Body*

The purpose of postural regulation is to keep the plane of the body normal to the gravitational direction. Any inclination of the body is detected by a posture sensor. The sensor is made up of a pendulum in an oil damper and a pair of electrodes. When the body inclines and the pendulum touches one of the electrodes, the contact signal produces a command for the supporting legs to execute a minute extention or retraction to recover from the inclined posture.

For the PANTOMEC to realize the GDA principle discussed in the previous section, the body should always be kept horizontal. Thus, posture control is essential. Horizontal posture is also desirable for the conveyance of passengers or a payload. The pendulum-type sensor performs adequately for statically stable low-speed walking, but for superior performance a gyroscope may be necessary.

3.2.3. *Leg-Adhering Regulation in the Four-Leg Standing Phase*

The standing posture with four legs is statically indeterminate, unlike the standing posture with three legs. Leg-adhering regulation requires that the weight of the body be distributed uniformly on the four legs. In a study of a six-legged walking vehicle, a control algorithm utilizing linear programming was introduced (Orin 1976).

In the present study, a very simple form of regulation was used, in which a leg is made to perform a minute downward motion whenever the sole of the foot leaves the ground. The regulation becomes effective when combined with the regulation of body height and posture described in Sections 3.2.1 and 3.2.2. For example, when one of the four supporting legs is forced off the ground by disturbances, such as the wind, the leg moves downward owing to this leg-adhering regulation; however, the delay of the command or structural compliance usually produces a deviation in body height and inclination. These deviations are corrected by the combined action of posture and body-height regulation. As a result of quasi-simultaneous implementation of all three types of regulation, the walking vehicle maintains stable posture in the four-legged supporting phase.

3.2.4. *Mode Regulation of the Supporting Phase*

Mode regulation determines the transition of the supporting phase. Regulation is indicated by the control command δ. $\delta = 0$ signifies the four-legged supporting phase. $\delta = i$, $i = 1, 2, 3, 4$, indicates the three-legged supporting phase with the ith leg in the swing phase. When command $\delta = i$ is transferred to $\delta = 0$, the following sequence is executed:

1. Lower the ith leg until the sole contacts the ground.
2. In the case that the sole does not contact the ground, lower the height of the body within the limits of its adjustable range.
3. If the sole does not contact the ground following steps 1 or 2, the vehicle stops moving. If the sole contacts the ground, the leg's downward motion stops and simultaneous backward motion of the four legs continues while $\delta = 0$ remains in effect.

3.2.5. *Obstacle-Avoidance Regulation*

When the swing leg contacts an object while swinging, and a signal is supplied by the tactile sensor shown in Fig. 5, the following sequence is executed:

Fig. 5. Tactile sensors on the sole.

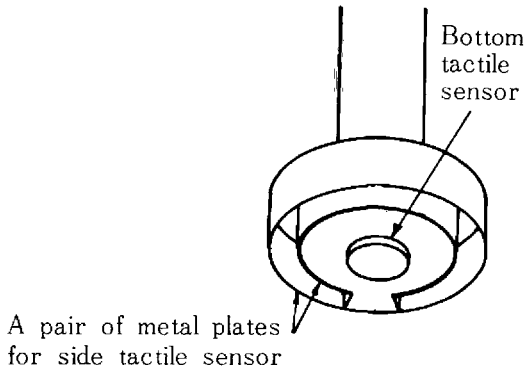

Fig. 6. Probing motion of the swing leg to avoid obstacles.

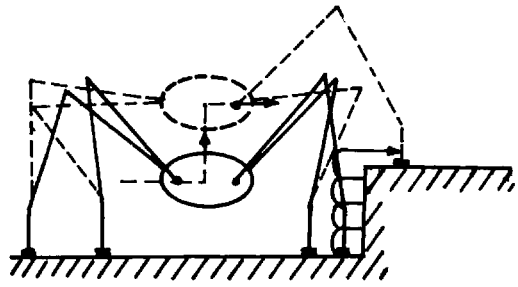

1. The swing leg recedes a certain distance in the direction opposite to the swing movement.
2. The height Z_i of the swing leg is raised to $Z_i + \Delta Z$.
3. If the height $Z_i + \Delta Z$ is over the motion limit of the swing leg, the height of the body is then raised within the limits of its adjustable range.
4. If, after steps 2 and 3, the swing leg cannot achieve height $Z_i + \Delta Z$ the vehicle stops; if height $Z_i + \Delta Z$ is achieved, then the original control sequence is reexecuted and the leg continues to swing.

As a result of the above sequence, the legs execute the obstacle-avoidance motion shown in Fig. 6.

The side-sole tactile sensor, composed of the pair of concentric metal plates shown in Fig. 5, is a 1-bit on/off switch and does not have the ability to distinguish the direction of contact. Thus, the direction of the receding motion of step 1 is simply opposite to the previous swing movement.

3.2.6. Velocity Regulation of Leg Motion

Velocity regulation is performed by changing the interval of transmission of the reference signal from the computer to each actuator servomechanism.

3.3. Walking Experiments with the PVII Quadruped Vehicle

The validity of the design criteria and the controlling algorithm have been demonstrated through experiments using the PVII quadruped vehicle. A visual sensor has not yet been installed. Thus, in the present control experiments, the gait command of level B (see Fig. 9) is fixed, that is, programmed by the operator from the beginning. The main purpose of the experiments is to examine the operation of the reflex-motion regulation (level C of Fig. 9).

In the first experiment, the PVII vehicle walked on even ground (see Fig. 4). Walking was implemented by the fundamental crawl-gait control. In tests with a 2-kg payload and a speed of 2 cm/s, the PVII showed an average power consumption of 10 W; this corresponds to a specific resistance of type 4, ϵ^*, of 25.5. The energy efficiency is low, but it is better than that of other experimental walking vehicles constructed thus far. During the walking sequence, a slight inclination of the body occurred at the moment of transition from the four-legged standing phase to the three-legged phase, but this inclination of the body was corrected by postural regulation at level C (see Fig. 9).

An object less than 18 cm in height was then placed on the floor to disturb the walking motion. It was observed that the vehicle stopped moving when the swing leg contacted the object, probed the object as shown in Fig. 6, and stepped over it. This experiment shows that the walking vehicle exhibits some adaptability even when operating under fixed-playback control at level B. Moreover, the walking vehicle has exhibited the ability to walk on stairs with arbitrary step height and length, as shown in Fig. 4C, under the same crawl-gait command.

Once the motion regulation of level C is shown to operate properly, the geometric position of the supporting legs can be commanded at level B without regard to the motion regulation of each step. Thus, the future expansion of gait control at level B becomes feasible.

Fig. 7. Model of quadruped walking vehicle.

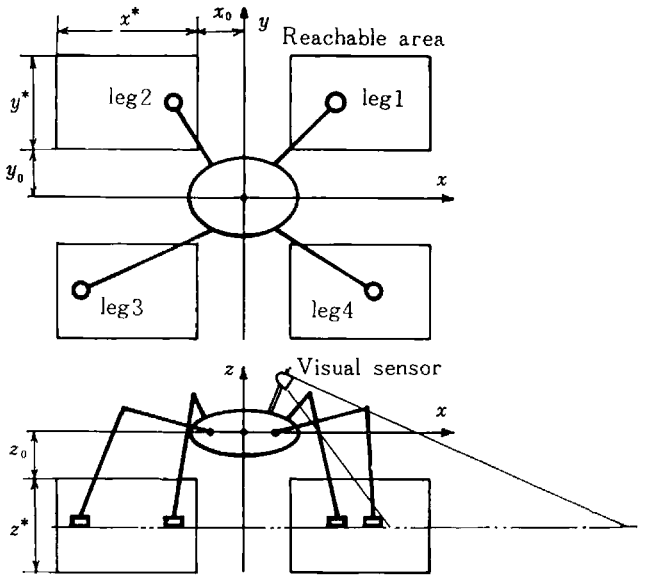

Other experiments were also performed by changing the gait command of level B, such as walking in the reverse direction, walking sideways, turning on the same spot, and turning while walking. However, continuous body motion was demonstrated only when the body was suspended to reduce the weight, because of frictional resistance in the simply designed bearing system and low output power of the dc motors in slow motion. More attention will be required in the design of future models in this respect.

The memory required by the motion-regulation and gait-control system is only about 5 Kbytes, owing to the Cartesian-coordinate-type motion of the PANTO-MEC leg systems.

4. Gait Control

4.1. Formalization of the Gait-Control Problem

In Section 3, results concerning the energy efficiency of walking motion, design criteria for leg geometry, and a description of a constructed quadruped walking vehicle were presented. Having described the practical feasibility of a walking vehicle, this paper will now address the adaptive gait-control problem. In this section, a formalization of the quadruped gait-control problem is given.

4.1.1. Qudaruped Walking Vehicle

The quadruped walking vehicle is modeled as shown in Fig. 7. The origin of the body-coordinate system is the body's center of gravity, and the body is assumed to align with the x-axis. The legs are numbered corresponding to the quadrant of the x-y plane in which they lie. Because a leg mechanism that permits Cartesian-coordinate-type motion, such as the PANTO-MEC, is assumed, each leg, i, has a rectangular solid reachable volume V_i, which is specified by six parameters: x_0, y_0, z_0, x^*, y^*, and z^*, as shown in Fig. 7. The projection of the reachable volume into the x-y plane is a rectangle denoted by R_i. The body is assumed to be kept horizontal during walking.

The installation of a visual sensor in the walking vehicle is anticipated. Therefore, short-range (approximately 30 steps) map information is assumed to be supplied to the gait controller.

4.1.2. Environment

Several discussions are available on the identification of the diverse, uneven terrain that walking vehicles may encounter in application (e.g., Bekker 1969). Here, a simplified five-type classification scheme is used, as shown in Fig. 8 (Hirose, Iwasaki, and Umetani 1982). The O-type terrain is ground on which regular walking can be realized without hindrance. It does not necessarily have a flat surface; as the reachable height z^* of the walking vehicle increases, increasingly uneven terrain becomes O-type terrain. H-type terrain is O-type terrain with depressions, such as holes or ditches. The walking vehicle cannot place a foot in a depression. P-type terrain is O-type terrain with protrusions, such as poles or rocks. The walking vehicle may not place a foot on a protrusion, nor may any part of the vehicle cross over a protrusion. HP-type terrain is a combination of H-type and P-type terrains. G-type terrain is general terrain with discrete cells.

Processing of information from the visual sensor is assumed to be as follows:

Fig. 8. Classification of terrain.

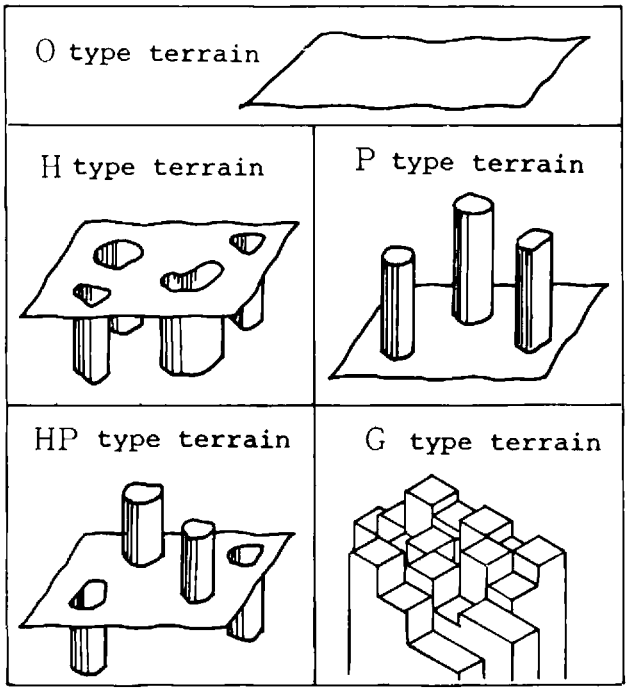

1. Form a G-type-terrain map by using information from the visual sensor.
2. Classify the G-type terrain into other types of terrain by comparing the terrain map to the size of the legs' reachable volume.

This paper discusses the gait-control problem specifically on H-type terrain.

4.1.3. Structure of the Control System

The total control system of the quadruped walking vehicle has the hierarchical structure shown in Fig. 9. The main elements of the hierarchy are:

Level A: navigation planning
Level B: gait control
Level C: basic motion regulation

Some of the basic research on level C, which involves the function corresponding to reflex motion in a biological system, has been discussed in the previous section. Level B is partitioned into two sublevels: level B_1, a local motion-trace generator; and level B_2, an adaptive gait controller. Only level B_2 is discussed here.

The objective of current research is to complete study of levels B and C and to realize an intelligent gait-control system at these levels. Research at the A level is deferred until satisfactory performance is achieved by the B- and C-level subsystems. Metaphorically speaking, the current objective is to realize "horse intelligence" in the horse-rider relationship. The rider, having level-A intelligence, rides the horse by giving general commands of direction and speed. The horse follows the rider's commands, but when it recognizes such obstacles as ditches or rocks, it voluntarily modifies the given trajectory and adjusts its gait and posture. When the walking vehicle achieves the same level of performance as an "artificial horse," it will be an off-road transporter with controllability equal or superior to a conventional automobile.

4.1.4. Definitions and Notation

Definition 1: The *duty factor,* β, is the fraction of the locomotion cycle during which each leg is in contact with the supporting surface (McGhee and Frank 1968).

Definition 2: *Crab walking* is defined as walking motion with the direction of locomotion different from, or equal to, the longitudinal axis of the vehicle's body. The angle between the longitudinal axis and the direction of motion is the crab, denoted by α. In the case of $\alpha = 0^0$, the crab walking corresponds to straightforward walking.

Definition 3: The *stroke length,* λ^*, of a leg is the distance that the leg swings during one swing phase.

Definition 4: The *longitudinal stability margin, s,* is defined as the shortest distance from the body's center of gravity to the boundary of the support pattern, as measured in the direction of travel (McGhee and Frank 1968).

Definition 5: The *cycle time, T,* of a periodic gait is the time required for the completion of one cycle of locomotion.

Definition 6: A *step* is the interval from the time one swing leg is placed to the time the next swing leg is placed. One cycle of a periodic gait is thus divided into four steps for a quadruped.

Fig. 9. Flowchart of the overall control system of a walking vehicle.

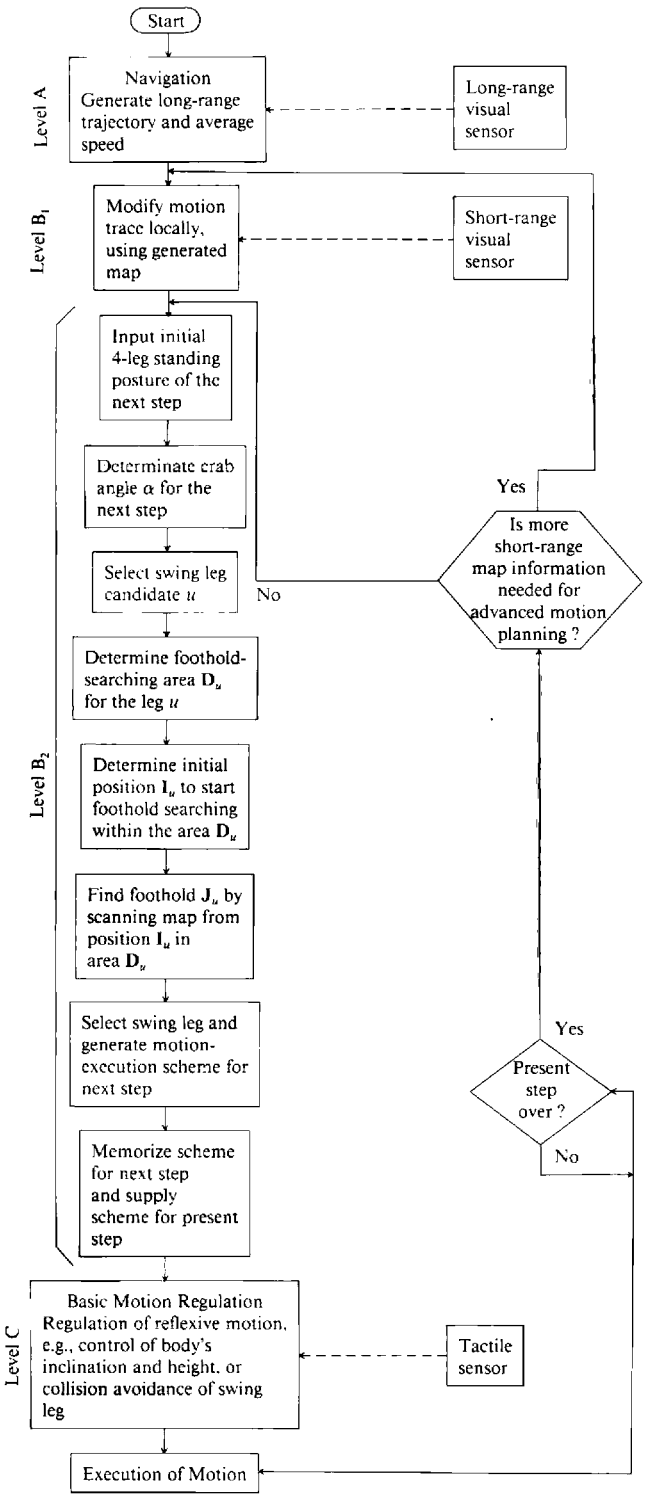

Definition 7: Point $\mathbf{P}_i$ ($i = 1, 2, 3, 4$) is the position of the bottom of the foot of leg i, measured in the body-coordinate system. In the same way, point $\mathbf{P}_a$ is defined as the point characterized by symbol a. x_a and y_a denote the x- and y-coordinates of $\mathbf{P}_a$, respectively.

Definition 8: $\mathbf{L}(\mathbf{P}_a, \mathbf{P}_b)$ denotes the line which passes through points $\mathbf{P}_a$ and $\mathbf{P}_b$.

Definition 9: The real valued functions $\mathbf{D}_x$, $\mathbf{D}_y$, and $\mathbf{D}_\alpha$ are defined as follows:

$$\mathbf{D}_x(\mathbf{P}_a, \mathbf{P}_b) = x_a - x_b.$$
$$\mathbf{D}_y(\mathbf{P}_a, \mathbf{P}_b) = y_a - y_b.$$
$$\mathbf{D}_\alpha(\mathbf{P}_a, \mathbf{P}_b) = \mathbf{D}_x(\mathbf{P}_a, \mathbf{P}_b)\cos(\alpha) + \mathbf{D}_y(\mathbf{P}_a, \mathbf{P}_b)\sin(\alpha).$$

Definition 10: The values g_i^x and g_i^y denote the maximum distance that the body's center of gravity can move as determined by the mechanical limitations of the ith leg.

Definition 11: The symbols f, r, $\bar{f}$, and $\bar{r}$ are used to indicate legs relative to a designated leg i. The letter f indicates a front leg, and r indicates a rear leg. $\bar{f}$ and $\bar{r}$ indicate the front and rear legs on the opposite side of the vehicle from leg i. For example, if leg 1 is designated ($i = 1$), then $f = 1$, $r = 2$, $\bar{f} = 4$, and $\bar{r} = 3$.

4.2. Adaptive Gait Controller (Level B_2)

In the adaptive gait controller of level B_2, it is assumed that a motion trace, along which the body's center of gravity should travel, is explicitly given by a higher-level subsystem (level B_1). The vehicle is assumed to execute crab walking. This means that the body axis of the vehicle is always kept parallel to the direction of the trajectory generated at level A while the vehicle follows the motion trace generated at level B_1.

One of the examples is shown in the simulation result of Fig. 18. Here, the x-axis is the trace planned at level A while the vehicle follows the motion trace generated at level B_1 and goes around an obstacle. This motion planning is adopted to exclude excessive rotational motion of the body at a locally adjusted trajectory. Crab walking is thus considered a basic mode of locomotion.

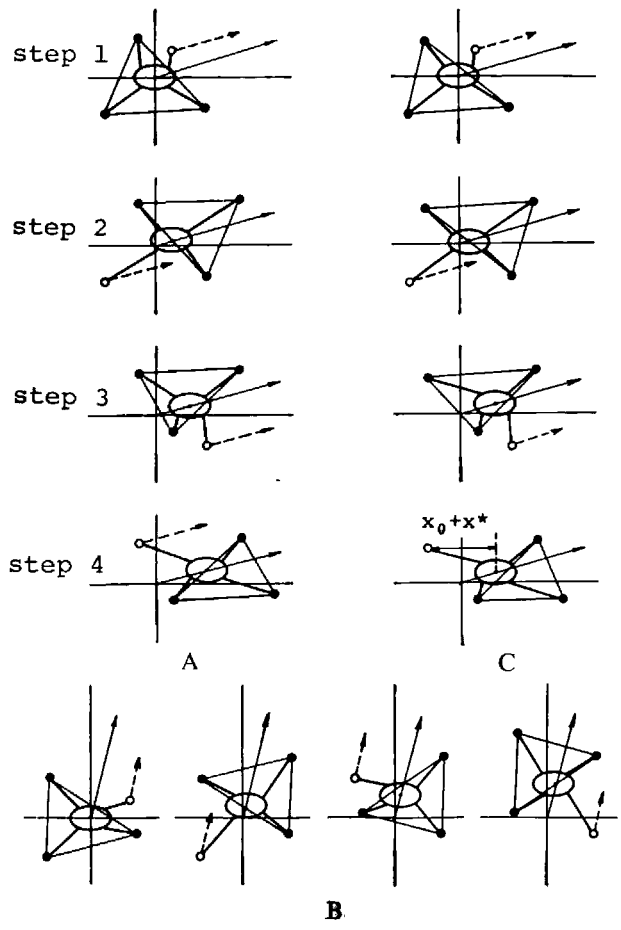

Fig. 10. Crab walking leg sequence. A. x-directional standard crab gait ($\alpha = 16°$). B. y-directional standard crab gait ($\alpha = 74°$). C. Crab walking ($\alpha = 16°$) started from an arbitrary posture and swinging each leg by its maximum stride, λ^*.

The motion planning of the gait is assumed to be carried out for the state one step in advance. Thus, as soon as the execution of the present step is completed, the next step can begin using the generated motion plan.

In the adaptive-gait-control algorithm, two objectives are incorporated. One is to select a "free gait" (Kugushev and Jaroshevskij 1975; McGhee and Iswandhi 1979) that accommodates to irregularities in the terrain; the other is to maintain the standard gait that exhibits maximum stability and highest efficiency, and admits continuous body motion, so far as terrain features permit. In short, the algorithm is to select a gait that best realizes both the high efficiency and the adaptability of walking motion, in accordance with terrain conditions. The sequence of steps that makes up the adaptive-gait-control algorithm (level-$\mathbf{B}_2$ control) is shown in Fig. 9, along with the other steps that constitute the remainder of the walking vehicle's control system. Details of each step in the adaptive-gait-control algorithm are discussed below.

4.3. Standard Gait

As pointed out by Wilson (1966), a *wave gait* is the standard gait in straightforward walking. Its pattern has already been identified (McGhee and Frank 1968). The most efficient wave gait for a quadruped vehicle is the crawl gait. The standard crab gait has not yet been considered, however. In the adaptive-gait-control algorithm of this paper, crab walking is often used. Therefore, the standard gait for crab walking will now be derived. The crawl gait discussed thus far is, of course, included in crab walking, as the special case of crab angle $\alpha = 0°$. In the derivation, only the projection of the gait pattern onto the x-y plane is considered.

The configuration of the vehicle is symmetric with respect to both the fore-aft and lateral axes; thus, it is sufficient to determine the standard crab gait for a crab angle α in the range $0 \leq \alpha \leq 90°$.

In order to specify the standard gait pattern, some constraints should be imposed on the leg's stroke trajectory. The analysis of foot motion in walking suggests that the stroke trajectories of the four legs should be symmetric about the body's center of gravity, provided that static stability can be maintained. Even with symmetry about the body's center of gravity, there can be a great deal of variation among the possible stroke trajectories. An additional restriction is, therefore, placed on the standard gait: the trajectory of each leg must pass through the central point $\mathbf{C}_i$ of the reachable area $\mathbf{R}_i$. (In three dimensions, the trajectory must pass through the vertical line in $\mathbf{V}_i$ that contains the point through $\mathbf{C}_i$.) In addition to simplifying the choice of trajectories, computer-simulation studies indicate that this requirement is flexible enough to permit standard gait walking at all crab angles.

Figure 10A shows the standard pattern for crab walking at a crab angle of $\alpha = 16°$, which is seen to be a modification of the x-directional crawl gait, or crab walking with $\alpha = 0^0$. The swing-leg sequence is 1-3-4-2. Figure 10B shows the pattern for $\alpha = 74°$, and is a modification of the y-directional crawl gait, or crab

walking with $\alpha = 90°$. In this case, the swing-leg sequence is 1-3-2-4. The difference in the swing-leg sequences suggests the existence of a critical angle α_c, where the standard leg sequence for crab walking changes from the x-directional sequence to the y-directional sequence. The x-directional gait pattern is maintained as long as such motion can be executed without any of the legs being moved across the axis of the body's motion trace. Therefore, the critical angle α_c is determined by the point $\mathbf{C}_i$ and expressed as

$$\alpha_c = \tan^{-1}((y_0 + y^*/2)/(x_0 + x^*/2)). \quad (2)$$

The vehicle selects the x-directional gait pattern for crab angles in the range $0 \leq \alpha < \alpha_c$ and the y-directional gait pattern for $\alpha_c < \alpha \leq 90°$. In the case $\alpha = \alpha_c$, both the x-directional and the y-directional gait are permitted, but the body's center of gravity moves along the periphery of the supporting-leg triangle, and the vehicle is least stable.

The stroke length λ^* of a leg is given by the formula

$$\lambda^* = \begin{cases} x^*/\cos(\alpha) \text{ for } 0° \leq \alpha \leq \tan^{-1}(y^*/x^*) \\ y^*/\sin(\alpha) \text{ for } \tan^{-1}(y^*/x^*) \leq \alpha \leq 90°. \end{cases} \quad (3)$$

The x- and y-directional distance traversed by the body's center of gravity, ΔG_x and ΔG_y, in one step are then expressed as

$$\begin{cases} \Delta G_x = ((1/\beta) - 1)\lambda^* \cos(\alpha), \\ \Delta G_y = ((1/\beta) - 1)\lambda^* \sin(\alpha). \end{cases} \quad (4)$$

These relations are illustrated in Fig. 11. In Fig. 12, the relative leg motion for one period of the x-directional standard gait is schematically illustrated.

4.4. Swing-Leg Selection

The swing-leg-selection algorithm is shown in Fig. 13. The algorithm is divided into two sections: (1) the tentative swing-leg selection before the foothold calculation and (2) the final selection of the swing leg made after the foothold calculation. Just after the crab angle α for the next step is determined, the algorithm searches in the final four leg-support patterns of the present step for a relative foot-positioning pattern that accords even partly to that of the standard gait for a

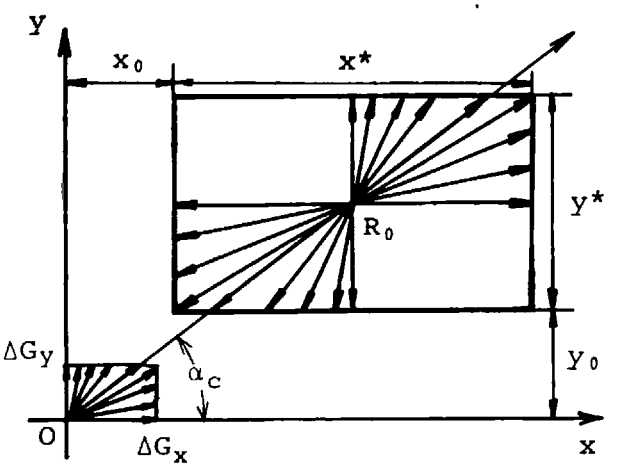

Fig. 11. The standard stroke motion of a leg at various crab angles.

crab angle α at the starting posture of the next step. If such a pattern is found, the leg that will maintain the geometric pattern of the standard crab gait is selected as swing-leg candidate u for the next step.

If no such swing-leg candidate is found, or if the foothold calculation reveals that candidate u cannot be swung forward, then a foothold calculation is carried out for each leg, and the leg with the longest swing is selected.

The selection procedure thus attempts to maintain a standard gait, or, failing that, efficiency of motion in a nonstandard gait.

4.5. Foothold Search Area $\mathbf{D}_u$

After a swing-leg candidate u is determined, a foothold search area, $\mathbf{D}_u$ must be computed. In this calculation, the body's center of gravity is assumed to lie in the forwardmost traversable position of the next step. The motion of the body's center of gravity is limited by the mechanical limitations of the support legs.

At first, it appears that the entire swing-leg-reachable area, $\mathbf{R}_u$, should be defined as $\mathbf{D}_u$ so as to make the most of the leg's adaptability to irregular terrain. However, previous research has revealed several weaknesses in this choice of $\mathbf{D}_u$. Figure 10A, for example, shows a standard x-directional crab walk in which the swing leg is always moved to the end of the reachable area. When this process is repeated from a slightly

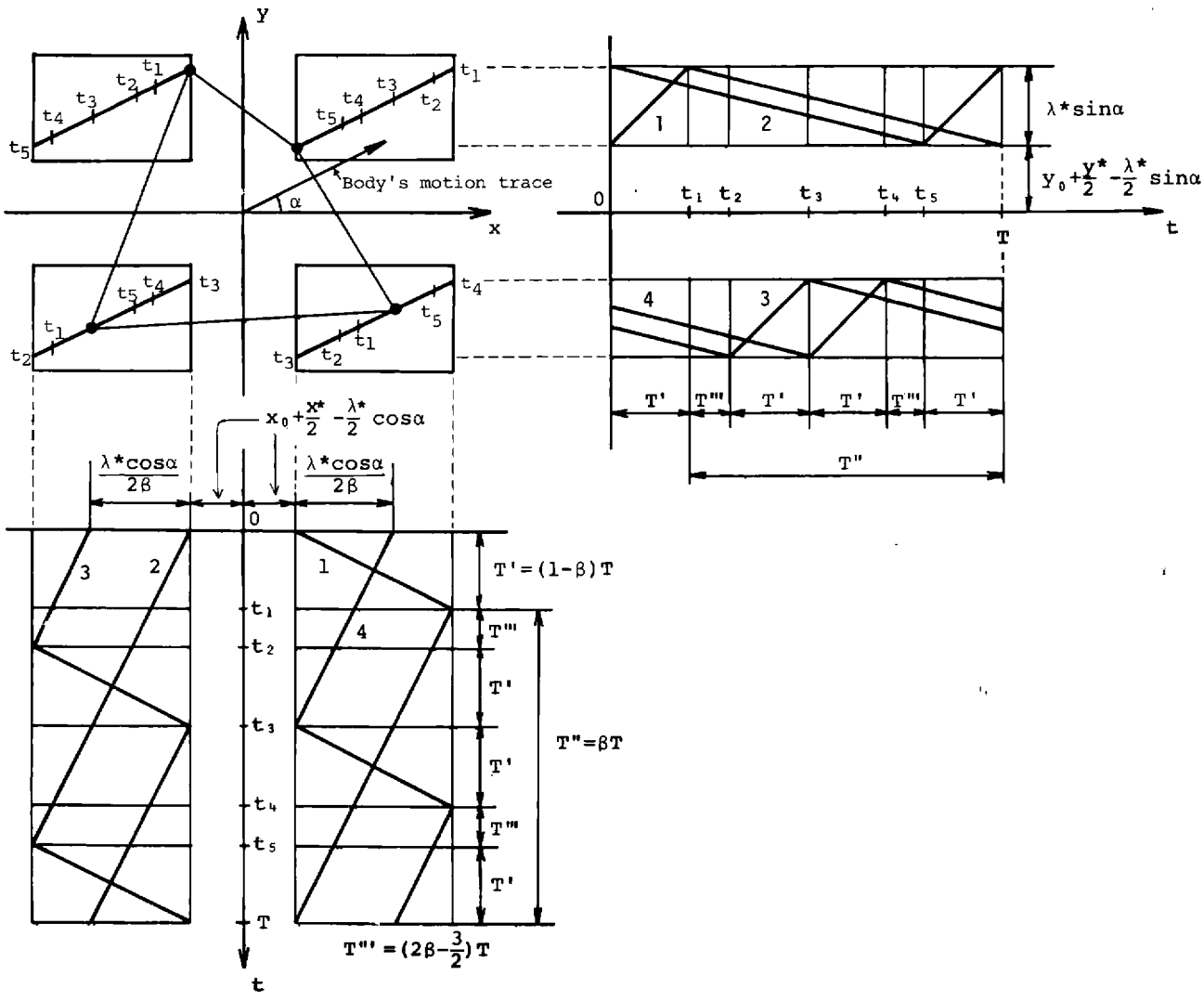

Fig. 12. Relative foot positioning in an x-directional standard crab gait. A. Foot motion in the x-y plane. B. Foot motion along the y-axis. C. Foot motion along the x-axis.

different initial leg position, as shown in Fig. 10C, the result is that (forward) walking motion cannot be maintained at the fourth step. Note that the deadlock occurs even if the terrain is perfectly flat.

This example reveals the importance of properly selecting the foothold search area $\mathbf{D}_u$. Research has revealed that a combination of three selection criteria is sufficient to avoid such deadlocked positions. These three criteria are referred to as diagonal principles I, II, and III.

4.5.1. Diagonal Principle I

Consider the deadlocked foot positioning in step 4 of Fig. 10C. In this posture, leg 2 must be advanced in order to permit the body to move forward along its motion trace; yet the body's center of gravity is not inside the supporting triangle formed by the other three supporting feet (thus leg 2 cannot be lifted). This is why the vehicle is halted at step 4.

The problematic foot positioning actually originated

Fig. 13. Swing-leg-selection algorithm.

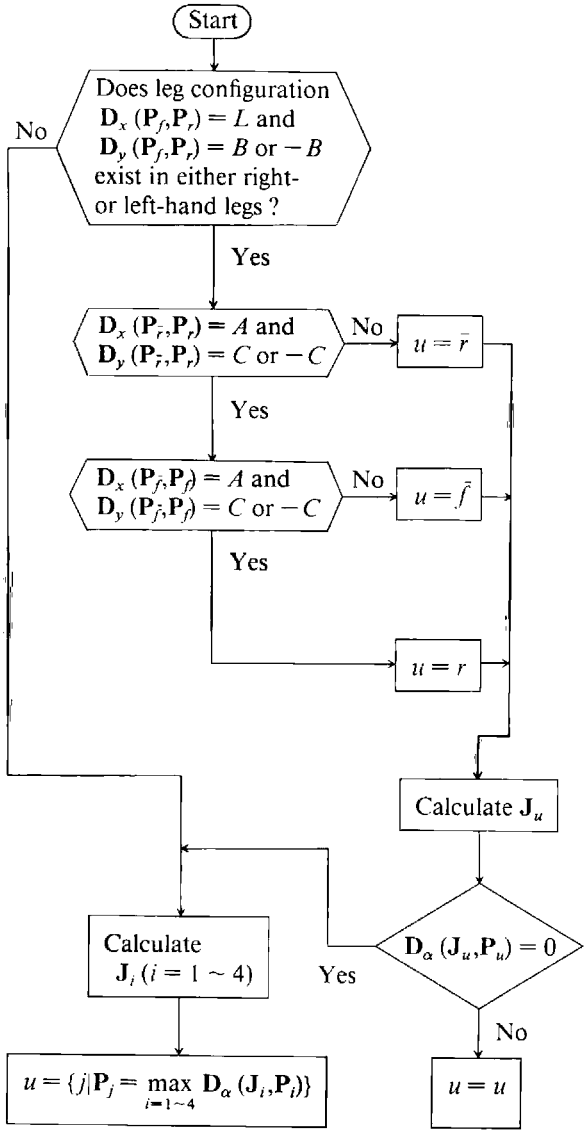

$$\begin{pmatrix} L = 2x_0 + \dfrac{\lambda^* \cos\alpha}{2\beta} & A = \dfrac{\lambda^* \cos\alpha}{2\beta} \\ B = \dfrac{1-\beta}{\beta}\lambda^* \sin\alpha & C = 2y_0 + \dfrac{2\beta - 1}{2\beta}\lambda^* \sin\alpha \end{pmatrix}$$

Fig. 14. Illustration of a part of diagonal principles I, II, and III.

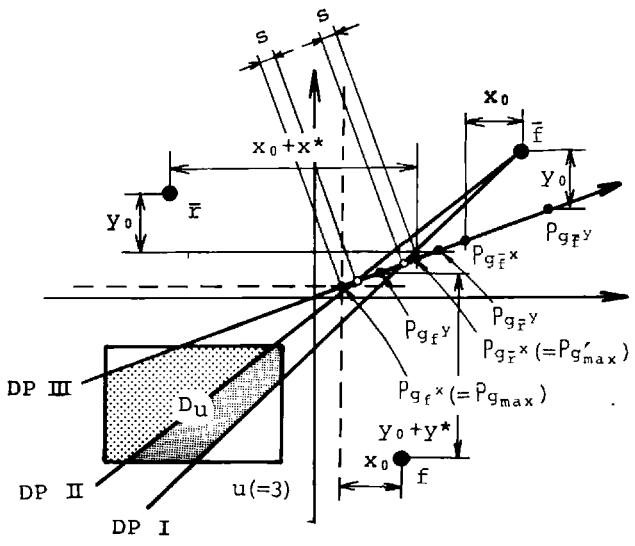

two steps earlier when leg 3 was moved. The deadlock can thus be prevented if the maximum reachable distance of leg 2 is considered at the time the foothold position of leg 3 is decided. This is the basic concept of diagonal principle I. From a simulation study, it was determined that this principle is needed only for the rear legs, that is, legs 2 and 3.

The action of diagonal principle I is to restrict the forward swing of a rear leg u so that the body's center of gravity remains in the supporting triangle $uf\bar{f}$ formed by the foot u and the two front feet. This is achieved by simply requiring that the body's center of gravity lie ahead of line $\mathbf{L}(\mathbf{P}_u, \mathbf{P}_{\bar{f}})$ (the line joining foot u and foot $\bar{f}$) by a longitudinal stability margin s. Diagonal principle I takes into account the geometric limitations of legs $\bar{f}$, $\bar{r}$, and u itself. The action of diagonal priciple I, shown in Fig. 14, is explained by the following.

The maximum distance, $g^x_{\bar{f}}$, that the body's center of gravity can traverse along its motion trace while the x-directional geometric limit of leg $\bar{f}$ is applied is derived from the relation

$$\mathbf{D}_x(\mathbf{P}_{\bar{f}}, \mathbf{P}g^x_{\bar{f}}) = x_0,$$

which yields

$$g^x_{\bar{f}} = (x_{\bar{f}} - x_0)/\cos(\alpha). \tag{5}$$

Similarly, $g^y_{\bar{f}}$, $g^x_{\bar{r}}$, and $g^y_{\bar{r}}$ can be shown to have the values

$$g^y_{\bar{f}} = \{y_{\bar{f}} + \text{sgn}\,(\bar{f} - 2.5)y_0 + 0.5(\text{sgn}\,(\bar{f} - 2.5) + \text{sgn}\,(\alpha))y^*\}/\sin(\alpha), \quad (6)$$

$$g^x_{\bar{r}} = \{x_{\bar{r}} + x_0 + x^*\}/\cos(\alpha), \quad (7)$$

$$g^y_{\bar{r}} = \{y_{\bar{r}} + \text{sgn}\,(\bar{r} - 2.5)y_0 + 0.5(\text{sgn}\,(\bar{r} - 2.5) + \text{sgn}\,(\alpha))y^*\}/\sin(\alpha), \quad (8)$$

The maximum distance $g'_{\max}$ that the body's center of gravity can move along its motion trace while the geometric limits of legs $\bar{f}$ and $\bar{r}$ are applied is

$$g'_{\max} = \min\,(g^x_{\bar{f}}, g^y_{\bar{f}}, g^x_{\bar{r}}, g^y_{\bar{r}}). \quad (9)$$

The foothold-search area of leg u is thus restricted to the rear of the line determined by $\mathbf{P}_{\bar{f}}$ and the forward-most point that the body's center of gravity can achieve on its motion trace (restricted by $g'_{\max} - s$, where s is the longitudinal stability margin defined in Section 4.1.4, and has a value of $(1 - 0.75/\beta)\cdot\lambda^*$ in the case of a standard crab gait with duty factor β). This region is the half-plane

$$x \leqslant \frac{(g'_{\max} - s)\cos(\alpha) - x_{\bar{f}}}{(g'_{\max} - s)\sin(\alpha) - y_{\bar{f}}}(y - y_{\bar{f}}) + x_{\bar{f}}. \quad (10)$$

It can be said that the forward motion of the body into the support triangle $u\bar{f}\bar{f}$ is guaranteed not to be interrupted by the geometric limitations of legs $\bar{f}$ and $\bar{r}$ provided that leg u is placed anywhere in the region (Eq. 10).

When the interruption of the geometric limitation of leg u itself is considered to drive the body's center of gravity into the support leg triangle $u\bar{f}\bar{f}$, the procedure to restrict the foothold-search area of leg u becomes a little more complicated.

Assume that leg 3 is going to be placed somewhere along the line $x = x_3$, as shown in Fig. 15. Let $\mathbf{G}_0$ be a point along the motion trace of the body's center of gravity that satisfies the relation

$$\mathbf{D}_x(\mathbf{G}_0, \mathbf{P}_3) = X_0 + x^* - s\cdot\cos(\alpha).$$

Then leg 3 should be placed behind the line $\mathbf{L}(\mathbf{P}_1, \mathbf{G}_0)$ to guarantee that the body's center of gravity will lie

Fig. 15. Loci of the point $\mathbf{P}_c$ (in diagonal principle I, based on the geometric limitation of leg u).

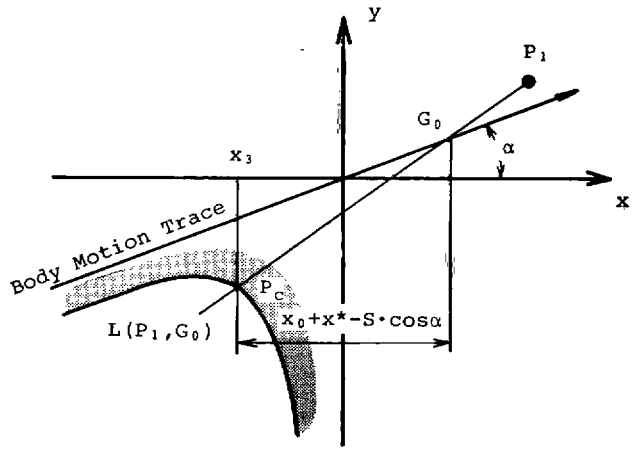

forward of the diagonal line $\mathbf{L}(\mathbf{P}_3, \mathbf{P}_1)$. Therefore, if leg 3 is placed somewhere on the line $x = x_3$, it should be placed to the left of the point $\mathbf{P}_c$, lying at the intersection of the line $x = x_3$ and the line $\mathbf{L}(\mathbf{P}_1, \mathbf{G}_0)$. As the position of x_3 is varied, the location of $\mathbf{P}_c$ sweeps out a hyperbolic curve, as shown in Fig. 15. The values of $\mathbf{P}_c = (x, y)$ satisfy the relation

$$(y - x\cdot\tan\alpha)(x - x_{\bar{f}} + dx_u) = (y_{\bar{f}} - x_{\bar{f}}\tan\alpha)dx_u, \quad (11)$$

where $dx_u = x_0 + x^* - s\cdot\cos\alpha$

By applying the same principle to the y-directional movement of the swing leg, another hyperbolic curve bounding the region of permissible footholds is

$$(y - x\cdot\tan\alpha)(y - y_{\bar{f}} + dy_u) = (y_{\bar{f}} - x_{\bar{f}}\tan\alpha)dy_u, \quad (12)$$

where $dy_u = \text{sgn}\,(u - 2.5)y_0 + 0.5(\text{sgn}\,(u - 2.5) + \text{sgn}\,(\alpha))y^* - s\cdot\sin\alpha$.

Equations (11 and 12) provide additional boundaries for the foothold-search area $\mathbf{D}_u$ when the interruption of the body's advance into the supporting triangle $u\bar{f}\bar{f}$ by the geometric limitation of leg u itself is considered. The exact expression of the permissible area within the boundaries derived above is not given here due to its complexity. However, it might be determined by analogy to the example shown in Fig. 16.

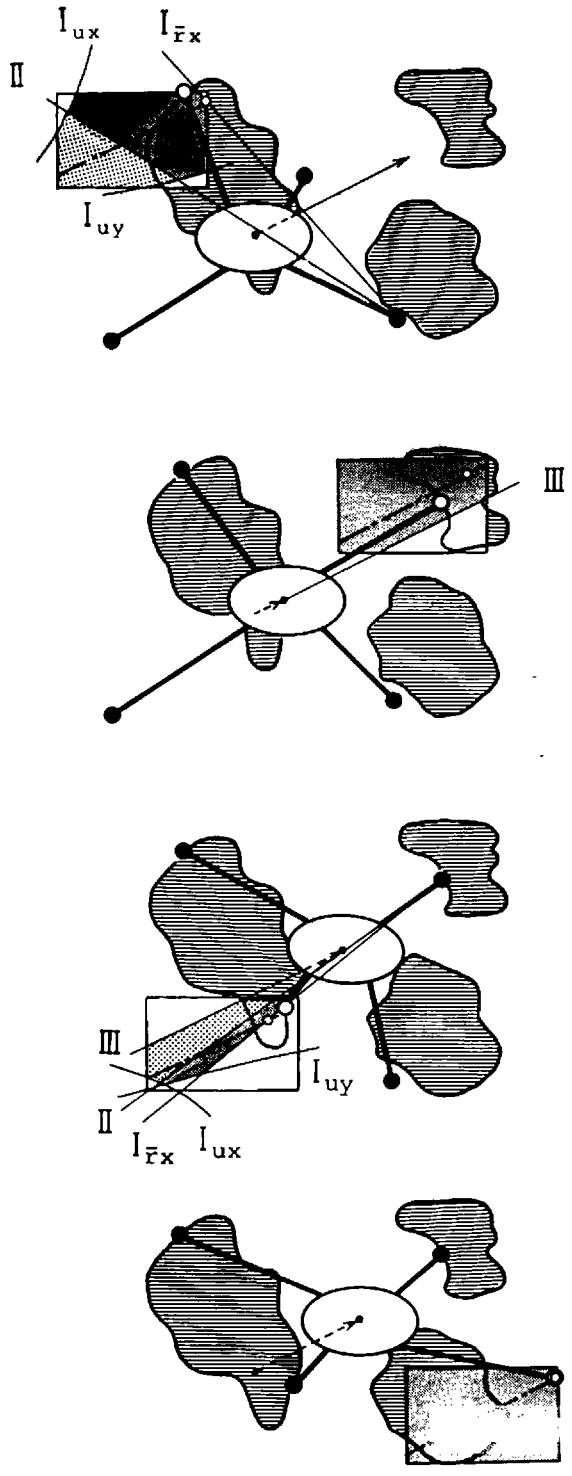

Fig. 16. Integrated procedure of the adaptive-gait-control sequence. $\alpha = 28°$; $\beta = 0.8$; $\mathbf{I}_{rx}$ indicates the diagonal principle I when the x-directional mechanical limit of leg r is applied.

4.5.2. Diagonal Principle II

Diagonal Principle II attempts to introduce a tendency to converge to the standard swing-leg sequence by taking into account the fact that leg f is swung just after leg u is placed in the standard sequence of the crawl gait. The principle is used when the current swing leg u is one of the rear legs ($u = 2$ or $u = 3$). The maximum distance g_{max} that the body's center of gravity can move along its motion trace while the geometric limits of legs f, $\bar{f}$, and $\bar{r}$ are applied is

$$g_{max} = \min \{g'_{max}, g^x_{\bar{f}}, g^y_{\bar{f}}\}, \tag{13}$$

where g'_{max} is as defined in (Eq. 9).

Diagonal principle II asserts that the area in front of the line joining $\mathbf{P}_f$, and the forward limit of the body's center of gravity on its motion trace with longitudinal stability margin s (limited by $g_{max} + s$) should be searched before the area behind the line, as shown in Fig. 14. The reason for this is that if a foothold for swing leg u is located forward of this line, then the body's center of gravity will remain in the triangle $\Delta u \bar{f} \bar{r}$ with a longitudinal stability margin s, and leg f can be moved in the next step.

Note that this principle only gives priority in searching order and does not exclude the area aft of the line altogether.

4.5.3. Diagonal Principle III

Although diagonal principles I and II are executed only for the rear legs, diagonal principle III is used for both rear and front legs. This principle is simple. Suppose, for example, that during crab walking the motion trace of the vehicle's body intersects the reachable area of leg 3, as shown in Fig. 14. Diagonal principle III excludes the area to the left of the motion trace from the foothold-search area for leg 3 and thus maintains the relative foot positioning of the crawl gait.

Diagonal principle III is applied in the foothold selections shown in Fig. 16B and C.

4.6. Initial Foothold-Search Position $\mathbf{I}_u$

The initial foothold-search position $\mathbf{I}_u$ is located inside the search area $\mathbf{D}_u$, and the search for foothold $\mathbf{J}_u$

Table 3. Δy and Δy for the Phase-Reserved Positioning Method

u	u^*	Δx	Δy
1	2	$2x_0 + \frac{3}{2}x^* + \left(\frac{1}{\beta} - \frac{3}{2}\right)\lambda^* \cos\alpha$	$\frac{\text{sgn}(\alpha)}{2}y^* + \left(\frac{1}{\beta} - \frac{3}{2}\right)\lambda^* \sin\alpha$
4	3		
2	4	$-2x_0 - \frac{1}{2}x^* - \frac{1-\beta}{2\beta}\lambda^* \cos\alpha$	$-\text{sgn}(u-2.5)\cdot(2y_0 + y^*) + \frac{\text{sgn}(\alpha)}{2}y^* - \frac{1-\beta}{2\beta}\lambda^* \sin\alpha$
3	1		

starts at this position. On level ground or O-type terrain, the position $\mathbf{I}_u$ is selected as foothold $\mathbf{J}_u$; therefore, the choice of $\mathbf{I}_u$ affects the ability of the algorithm to converge to a standard gait. The method used for determining $\mathbf{I}_u$ is referred to as phase-reserved positioning (PRP).

In the PRP method, the position of the leg that would be swung before the present swing leg u in the standard gait sequence pattern shown in Fig. 12, for example, is taken into consideration. Along the stroke trajectory of leg u, two points, $\mathbf{P}_{\Delta x}$ and $\mathbf{P}_{\Delta y}$, are located as follows: the quantities Δx and Δy are calculated from the formulas in Table 3, and then $\mathbf{P}_{\Delta x}$ and $\mathbf{P}_{\Delta y}$ are located along the trajectory of leg u from the requirements

$$\begin{aligned} \mathbf{D}_x(\mathbf{P}_{\Delta x}, \mathbf{P}_{u^*}) &= \Delta x, \\ \mathbf{D}_y(\mathbf{P}_{\Delta y}, \mathbf{P}_{u^*}) &= \Delta y. \end{aligned} \tag{14}$$

The initial search position $\mathbf{I}_u$ is then taken to be whichever of the points $\mathbf{P}_{\Delta x}$ and $\mathbf{P}_{\Delta y}$ is closest to the current position of leg u (Fig. 16B). If this value of $\mathbf{I}_u$ does not lie within the search area $\mathbf{D}_u$, then the foremost point along the stroke trajectory of leg u lying within $\mathbf{D}_u$ is selected as $\mathbf{I}_u$.

The PRP method is based on the idea of preserving the phase-shifted positioning relation between subsequent swing legs u and u^*. That is, when a leg u^* reaches the end of its support phase, the leg u, which is to be swung next, should maintain the stroke of the standard gait, $(1-\beta)\lambda^*$, so that the relative foot position of the standard gait is preserved. The PRP method attempts to realize this relation through the choice of the initial search position $\mathbf{I}_u$.

4.7. Foothold Decision and Subsequent Procedures

The foothold position $\mathbf{J}_u$ for swing leg u is located by scanning the area $\mathbf{D}_u$ beginning at location $\mathbf{I}_u$. There are several possible scanning methods. A simple method used in the algorithm is to partition $\mathbf{D}_u$ into rows and columns to form discrete cells, and then search the cells one row, or y-directional line, at a time, starting from a cell near the location $\mathbf{I}_u$. If $\mathbf{I}_u$ is contained in row k, then rows are searched in the order k, $k-1$, $k+1$, $k-2$, $k+2$, . . . , until a valid foothold is located.

After the position $\mathbf{J}_u$ is determined, the following operations are performed:

1. Select the swing leg u for the next step according to the algorithm shown in Fig. 13, and calculate the resultant distance to be traversed by the body's center of gravity.
2. If none of the legs can be swung forward, generate a motion plan to bring the body back. If a position is reached where, again, none of the legs can be swung forward, halt the vehicle.
3. Generate the motion-execution commands for each leg necessary to carry out the next step.

A detailed algorithm is necessary for operation 3 if smooth walking motion is to be realized. The design of such an algorithm is left for future research. After completing these three procedures, the gait controller executes one step of walking motion, as indicated by the flowchart in Fig. 9.

Fig. 17. Walking motion over a river using the proposed algorithm. (Step numbers are shown: $\beta = 0.75$.)

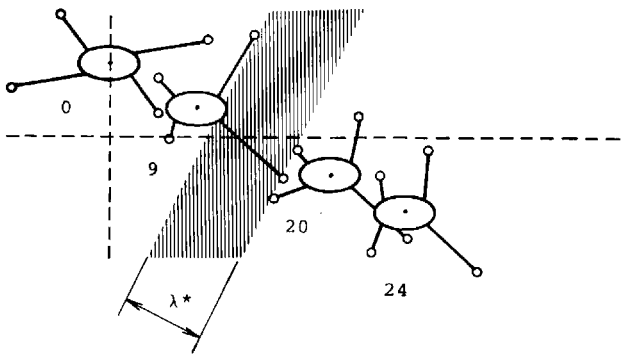

4.8. Simulation Study

Three simulation results are introduced as evidence of the validity of the above-described algorithm. Figure 16 shows a gait-sequence simulation on a sample of H-type terrain (see Fig. 8).

Figure 17 shows the walking motion used to stride over a broad depression, such as a river. The width of the river is λ^*, the maximum stroke distance of the legs at the given crab angle. Although the task looks puzzling, the vehicle automatically aligns the foot positions along the edge of the river, then strides across and returns to standard-gait crab walking.

Figure 18 shows a simulation on H-type terrain which has an untraversable hole lying on the motion trace generated by the level-A controller. In this example, a simplified level-B_1 controller was used to generate a simple modified motion trace to avoid the hole and traverse the terrain. This paper does not discuss the motion-trace modification procedure corresponding to level-B_1 control (in Fig. 9). The simulation study suggests that the present algorithm can be developed into an intelligent gait controller if it is combined with a sophisticated level-B_1 controller in the future.

5. Conclusion

In this paper, the energy efficiency of walking vehicles and the effect of leg geometry on efficiency was discussed. It was shown that a design that incorporates a pantograph mechanism can result in a lightweight, easily controlled leg. The specifications and the basic motion-regulation system of a constructed quadruped walking vehicle were described in detail. It was shown that the model has successfully demonstrated several modes of walking motion on uneven terrain and that these modes incorporate some adaptability.

The adaptive-gait-control problem was presented, with attention given to the case of a quadruped vehicle. A solution was presented that seeks to combine maintenance of an efficient gait on regular terrain with adaptability to irregular terrain and the avoidance of deadlocked positions. The solution, in algorithm form, has been tested in computer simulations and found to give good results.

It is emphasized that the study of walking vehicles is still in its infancy. Some important unsolved problems are

1. Detailed analysis of the energy efficiency of walking motion. A mechanism to absorb kinetic energy in oscillating motion of the legs or the introduction of variable-speed transmission for power matching of the driving system will have to be seriously considered.
2. Introduction of a rigid and lightweight leg and hull structure. A new material, such as carbon fiber reinforced plastic, is a likely choice. A study of structure and materials specifically for walking vehicles will have to be implemented.

As for the gait-control problem, many aspects of it are still unsolved. Some of these are

1. Generation of a locally modified motion trace corresponding to level-B_1 control (Fig. 9). The realization of a visual sensor is, of course, a critical problem.
2. Generation of smooth body motion during terrain-adaptive walking (level C of Fig. 9).
3. A detailed analysis of stability. In this paper, static stability (nonnegative stability margin) was made a requirement in the gait-selection procedure, but more research on the stability margin, or even the incorporation of dynamic stability, will have to be conducted.

The author previously divided the history of the study of walking vehicles into three phases. The fourth

Fig. 18. Adaptive walking on H-type terrain with local modification of the motion trace.

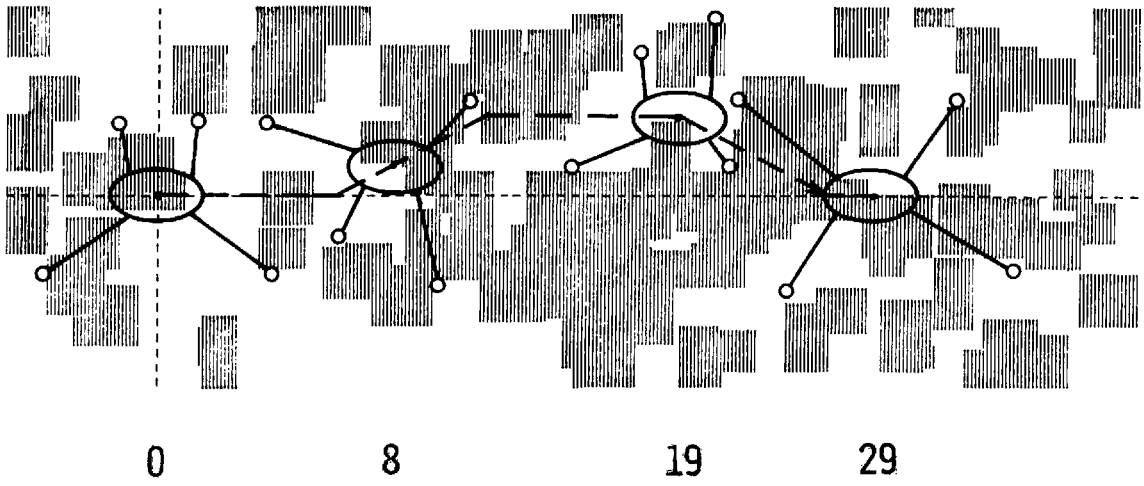

phase, still in the future, might be the emergence of walking vehicles with high-speed mobility achieved through dynamic walking together with improved energy efficiency and terrain adaptability. The author believes that, as far as the quadruped is concerned, there are several feasible methods to realize dynamic walking. Some research toward this end is already under way (Raibert 1981). Both theoretical and experimental studies of quadruped dynamic walking need to be advanced.

6. Acknowledgments

The author would like to express his gratitude to Mr. H. Iwasaki, Mr. M. Nose, and Mr. H. Kikuchi for their sincere cooperation in the execution of this study, and Prof. Y. Umetani for his warm understanding and support of the study.

References

Bekker, M. G. 1969. Introduction to terrain-vehicle systems. Ann Arbor: University of Michigan Press.

Gabrielli, G., and von Karman, I. 1950. What price speed? *Mechanical Engineering* 72(10):775–781.

Goldspink, G. 1977. Energy cost of locomotion. *Mechanics & energetics of animal locomotion,* ed. R. McN. Alexander and G. Goldspink. London: Chapman and Hall, pp. 153–167.

Hirose, S., and Umetani, Y. 1978 (Udine, Italy). Some considerations on a feasible walking mechanism as a terrain vehicle. *Proc. 3rd CISM-IFToMM Symp. Theory and Practice Robots and Manipulators.* Amsterdam: Elsevier, pp. 357–375.

Hirose, S., and Umetani, Y. 1979. The basic considerations of energetic efficiencies of walking vehicles (in Japanese). *Trans. Soc. Instrument Contr. Engineers* 15(7):928–933.

Hirose, S., and Umetani, Y. 1980*a*. Some considerations on leg configuration and locomotion properties of walking vehicles (in Japanese). *Biomechanism* 5:242–250.

Hirose, S., and Umetani, Y. 1980*b*. The synthesis of basic motion regulator systems for quadruped walking vehicles and its experiments (in Japanese). *Trans. Soc. Instrument Contr. Engineers* 16(5):747–753.

Hirose, S., and Umetani, Y. 1980*c*. The basic motion regulation system for a quadruped walking vehicle. ASME 80-DET-34. Paper delivered at ASME Conf. Mechanisms, Los Angeles.

Hirose, S., and Umetani, Y. 1981 (Tokyo). A cartesian coordinate manipulator with articulated structure. *Proc. 11th Int. Symp. Industrial Robots.* London: Internation Fluidics.

Hirose, S., Iwasaki, H., and Umetani, Y. 1982. The basic study of the intelligent gait control of quadruped walking vehicles (in Japanese). *Trans. Soc. Instrument Contr. Engineers* 18(2):193–200.

Hoppie, L. O., et al. 1979. The feasibility of an elastomeric regenerative braking system for automotive applications. Tech. Rept. UCRL-15037. University of California.

Ikeda, K., et al. 1973. Finite state control of quadruped walking vehicle—control by hydraulic digital actuator (in Japanese). *Biomechanism* 2:164–172.

Kugushev, E. I., and Jaroshevskij, V. S. 1975. Problems of selecting a gait for an integrated locomotion robot. Paper delivered at 4th Int. Conf. Artificial Intell. Tbilisi, Georgian SSR, USSR.

McGhee, R. B., and Frank, A. A. 1968. On the stability properties of quadruped creeping gait, *Math. Biosci.* 3(3):331–351.

McGhee, R. B., et al. 1978 (Udine, Italy). Real-time computer control of a hexapod vehicle. *Proc. 3rd CISM-IFToMM Symp. Theory and Practice Robots and Manipulators.* Amsterdam: Elsevier, pp. 323–339.

McGhee, R. B., and Iswandhi, G. I. 1979. Adaptive locomotion of a multilegged robot over rough terrain, *IEEE Trans. Syst. Man Cybern.* SMC-9(4):176–182.

Mosher, R. S. 1968. Test and evaluation of a versatile walking truck. *Proc. Off-Road Mobility Res. Symp.* Hanover, N.H.: International Society for Terrain Vehicle Systems, pp. 359–379.

Nakano, E., et al. 1982. Methodology of energy saving for autonomous mobile robots (in Japanese). *Biomechanism* 6:223–231.

Orin, D. E. 1976. Interactive control of a six-legged vehicle with optimization of both stability and energy. Ph.D. diss., The Ohio State University.

Park, F. 1962. Near surface vehicle. *International Science and Technology,* pp. 12–22.

Raibert, M. H. 1981 (Zaborow, Poland). Dynamic stability and resonance in a one legged hopping machine. *Proc. CISM-IFToMM Symp. Theory and Practice Robots and Manipulators.* Amsterdam: Elsevier, pp. 419–429.

Taylor, C. R. 1973. Energy cost of animal locomotion. *Comparative Physiology,* ed. L. Bolis, K. Schmidt-Nielsen, and S. H. P. Maddrell. Amsterdam: North-Holland, pp. 23–42.

Waldron, K. J., and Kinzel, G. L. 1981 (Zaborow, Poland). The relationship between actuator geometry and mechanical efficiency in robots. *Proc. 4th CISM-IFToMM Symp. Theory and Practice Robots and Manipulators.* Amsterdam: Elsevier, pp. 366–374.

Wilson, D. M. 1966. Insect walking. *Annu. Rev. Entomol.* 11:103–121.